# Characterization of the tyrosine phosphorylation and distribution of dystrobrevin isoforms

Sudha Balasubramanian[b], Eric T. Fung[b], Richard L. Huganir[a,b,*]

[a]*Howard Hughes Medical Institute, Johns Hopkins University School of Medicine, Department of Neuroscience, 725 North Wolfe Street, 904A PCTB, Baltimore, MD 21205-2185, USA*

[b]*Johns Hopkins University School of Medicine, Department of Neuroscience, 725 North Wolfe Street, 904A PCTB, Baltimore, MD 21205-2185, USA*

Received 8 June 1998

**Abstract** **Dystrobrevin, a member of the dystrophin family of proteins, was initially identified as a major tyrosine phosphorylated synaptic protein in the electric organ of *Torpedo californica*. In this paper, we show that the major sites of tyrosine phosphorylation of *Torpedo* dystrobrevin are within its C-terminus, on Tyr-693 and Tyr-710. Cloning of the mammalian homologue of dystrobrevin has recently shown that this phosphotyrosine containing tail, or PYCT, is subject to alternative splicing. To compare the expression and distribution of PYCT$^-$ and PYCT$^+$ splice variants, we generated antibodies against different regions of dystrobrevin. Here we show that the PYCT$^-$ isoform of 62 kDa is expressed at high levels in all tissues examined. In contrast, PYCT$^+$ isoforms are expressed primarily in brain and muscle, where they are concentrated at synapses. Moreover, PYCT$^+$ isoforms associate more tightly with the membrane and with syntrophin, another synaptically enriched protein. These results suggest that PYCT$^+$ isoforms of dystrobrevin are specialized components of the dystroglycan complex which render the complex sensitive to regulation by tyrosine kinases.**

**© 1998 Federation of European Biochemical Societies.**

*Key words:* Neuromuscular junction; Dystrobrevin; Tyrosine phosphorylation

## 1. Introduction

Synapses are areas of contact between cells which are highly specialized for the transmission of chemical signals [1]. To maximize sensitivity during signaling, neurotransmitter receptors and other proteins involved in signal transduction are concentrated precisely beneath the sites of neurotransmitter release. The synaptic cytoskeleton is thought to immobilize the signal transduction apparatus and hence maintain and modulate the structure of the synapse [2]. The electric organ of *Torpedo californica*, a modified cholinergic synapse and abundant source of synaptic proteins, has greatly facilitated the biochemical study of the synaptic cytoskeleton. Alkaline extracts of membranes prepared from this tissue are enriched in several proteins including rapsyn, syntrophin, dystrobrevin (formerly known as 87K) and dystrophin [3,4]. The functional importance of rapsyn is evident from the failure of neurotransmitter receptors and other synaptic proteins to cluster at the neuromuscular junctions (NMJs) of rapsyn deficient mice [5]. Although syntrophin, dystrobrevin and dystrophin have been shown to be part of a protein complex localized to the synapse [3,6–9], the roles of these proteins in synaptic function is less clear.

Dystrophin was first identified as the product of the Duchenne's muscular dystrophy gene [10]. It is a 427-kDa protein, expressed primarily in muscle, with several domains: an N-terminal actin-binding domain; a central rod domain containing a number of spectrin like repeats; and, finally, a cysteine rich C-terminus, referred to as the CRCT [11]. A complex of proteins, collectively termed the dystrophin-associated proteins, copurify with dystrophin isolated from rabbit skeletal muscle [12]. This complex includes several transmembrane proteins including the extracellular glycoprotein α-dystroglycan, which binds extracellular matrix proteins such as laminin [13], as well as several peripheral membrane proteins, including the rabbit homologues of syntrophin [14] and dystrobrevin [15].

The components of the dystrophin complex are encoded by multiple related genes which are subject to alternative splicing (reviewed in [16]). For example, in addition to dystrophin, which is itself subject to extensive alternative splicing, there exists the structurally analogous utrophin which also contains an actin binding domain, a spectrin repeat region and a CRCT [17]. The dystrophin family also includes dystrobrevin with its various splice isoforms [18–20], and the closely related protein β-dystrobrevin [21]. Similarly, three different syntrophin genes have been identified, at least two of which are subject to alternative splicing [22–24].

The various isoforms of the dystrophin complex show differential tissue expression. Interestingly, it appears that some isoforms are synapse specific. For example, in muscle, while dystrophin and α1- and β1-syntrophin are expressed throughout the sarcolemma, utrophin and β2-syntrophin appear to be restricted to the NMJ [9,21,25]. The extensive diversity of the dystrophin complex suggests that these complexes may have some specialized, regulated function which varies with cell type and subcellular location, particularly at the synapse.

The synapse contains specialized membrane and cytoskeletal domains which are assembled during synaptogenesis [26]. Reorganization of the post-synaptic membrane at the NMJ is induced by neuronal agrin, an extracellular matrix molecule released by the presynaptic nerve terminal and deposited in what becomes the synaptic basal lamina [27]. Studies using cultured muscle cells have shown that agrin induces the aggregation of the acetylcholine receptor (AChR) [28]. Such aggregation is accompanied by AChR tyrosine phosphorylation and is blocked by tyrosine kinase inhibitors [29,30]. Moreover, recent studies have shown that agrin regulates the activity of MuSK, a muscle-specific receptor tyrosine kinase that is essential for proper synapse formation [31,32]. These data suggest that tyrosine phosphorylation plays an

*Corresponding author. Fax: (1) (410) 955-0877.
E-mail: rick.huganir@qmail.bs.jhu.edu

0014-5793/98/$19.00 © 1998 Federation of European Biochemical Societies. All rights reserved.
PII: S0014-5793(98)00804-7

important role in the organization of the synaptic cytoskeleton at the NMJ.

One major phosphotyrosine containing component of the synaptic membranes from *Torpedo* is the dystrophin-associated protein dystrobrevin [18,33]. Analysis of the amino acid sequence of dystrobrevin reveals several tyrosine kinase consensus sites on the C-terminal tail (the phosphotyrosine containing tail, or PYCT), a region of the molecule subject to alternative splicing [19,20,33]. Because not all splice variants of dystrobrevin contain the PYCT, differential splicing could, in theory, confer tissue-specific sensitivity to extracellular signals mediated by tyrosine kinases.

In this study, we examine the function of the PYCT domain of dystrobrevin. First, we demonstrate that the two major sites of tyrosine phosphorylation of dystrobrevin are Tyr-693 and Tyr-710 – both of which are contained within the PYCT. We show that, while $PYCT^-$ isoforms are highly abundant and ubiquitously expressed in all tissues, $PYCT^+$ isoforms are expressed predominantly in brain and muscle where they are localized to the synapse. Moreover, $PYCT^+$ isoforms are more tightly associated with the membrane than $PYCT^-$ isoforms. Finally, $PYCT^+$ isoforms are associated with syntrophin to a greater degree than the $PYCT^-$ isoforms. Taken together, these results suggest that alternative splicing at the PYCT plays a role in regulating subcellular distribution of dystrobrevin and may regulate the sensitivity of dystrobrevin to tyrosine kinase mediated signaling.

## 2. Materials and methods

### 2.1. Materials

Post-synaptic membranes from electric organ were prepared as described previously [34]. Leupeptin, antipain, chymostatin, and pepstatin were obtained from Chemicon; aprotinin from Miles. All chemicals were obtained from Sigma unless otherwise noted.

### 2.2. Constructs

*Torpedo* dystrobrevin was polymerase chain reaction (PCR) amplified using the 5′ primer ACGCGTCGACAATGGTGAAAACTGCAGAAATGATTG and either the 3′ primer GAAGATCTTGTCAATGAATCTTGAGGTGTATG (myc-wt) or GAAGATGATCTTCACCCCTGCAAACTGACCTG (myc-ΔCT), and subcloned in frame into a PRK5 expression vector with a 5′ myc epitope tag.

Mutagenesis was performed using the Chameleon kit (Stratagene), according to the manufacturer's protocol using the following antisense primers: CATCTGTTCTAACAAAGCTTTCACCATCTTC (Y685F), GGACAGATTCATTTTCAAAGCTTTCATCATCTG (Y693F), GCAGTTTTTGTTTCAGGAATTCTTCCAGTTTTGACT (Y710F), or GTTCACCCCTGCAAGCTTACCTGAAAGTTCTCATCCTGCAG (Y720F); and the selection primer, GCCAGTGCCAAGCTGATATCAGCTTTTTGC. Mutagenesis was confirmed by sequencing.

To create the wild-type and mutant fusion proteins corresponding to the PYCT of dystrobrevin, the region corresponding to amino acids 604–726 of dystrobrevin was amplified from the myc-PRK5 dystrobrevin constructs. The resulting products were subcloned in frame into the vectors pGEX4T2 (WT, Y685F and Y710F) or pGEX2T (Y693F) from Pharmacia to create glutathione-*S*-transferase fusion proteins.

### 2.3. Fusion proteins

The fusion proteins were produced essentially as described [35]. Briefly, the constructs were transformed into *E. coli* strain BL21. An overnight culture was diluted 1:80, and grown to an OD of approximately 0.5. The culture was induced with 0.5 mg/ml IPTG (Gibco-BRL), and grown for an additional 4 h. The cells were harvested by centrifugation and resuspended in lysis buffer (PBS/5 mM EDTA/1 mM DTT/10 U/ml aprotinin) supplemented with additional protease inhibitors, or INH (0.1 mM phenylmethylsulfonylfluoride/10 μg/ml antipain, leupeptin, chymostatin and pepstatin). After sonication, Triton X-100 (BioRad) was added to 1%. The lysate was incubated on ice for 30 min, and centrifuged for 20 min at $700\times g$ at 4°C in an HS4 rotor. The supernatant was then adsorbed to glutathione agarose for at least 60 min. After extensive washing with lysis buffer, the agarose was eluted in lysis buffer and INH, with 10 mM reduced glutathione.

### 2.4. Antibodies

The anti-DHD polyclonal antiserum was generated against a glutathione-*S*-transferase fusion protein encoding amino acids 291–391 of *Torpedo* dystrobrevin as described previously [18]. The anti-PYCT antibody was made by injecting purified, dialyzed PGEX4T/WT fusion protein into New Zealand white rabbits (Hazelton). Both antibodies were affinity purified on fusion protein columns. Polyclonal antiphosphotyrosine antibodies were prepared as described previously [34]. Anti-syntrophin antibodies (MAb 1351) were a generous gift of Dr. Stanley Froehner.

### 2.5. Phosphorylation of post-synaptic membranes

Post-synaptic membranes, enriched in AChR and other post-synaptic proteins were prepared from *Torpedo californica* and phosphorylated in vitro, essentially as described in [18]. Postsynaptic membranes (10 mg) were incubated in 20 ml of phosphorylation buffer (20 mM Tris, pH 7.5, 20 mM $MgCl_2$, 2 mM $MnCl_2$, 1 mM EGTA, 1 mM EDTA, 1 mM ouabain, 1 mM sodium orthovanadate, 1 mM DTT, 1 μM Walsh protein kinase inhibitor peptide, and 20 μg/ml each of antipain, leupeptin, aprotinin, chymostatin and pepstatin). Phosphorylation was initiated with the addition of 50 μM [$\gamma$-$^{32}$P]ATP (2200 cpm/pmol). The reaction was allowed to proceed 60 min at 30°C.

Membranes were collected by centrifugation for 20 min at $66\,000\times g$ at 4°C, and resuspended by sonication in 5.8 ml of immunoprecipitation buffer, or IPB (PBS/5 mM EDTA/5 mM EGTA/10 mM sodium pyrophosphate/5 mM sodium fluoride (Mallinkrodt)/1 mM sodium orthovanadate). Triton X-100 was added to a final concentration of 1.3% and the membranes were incubated on ice for 20 min. The insoluble material was removed by centrifugation at $16\,000\times g$ in a refrigerated microcentrifuge. The supernatant was then incubated with 60 μl of anti-DHD crude antiserum or pre-immune serum and 900 μl of a 2× slurry of protein A-Sepharose in IPB+1% BSA for 3 h at 4°C. After washing 5 times with 6 ml of IPB+1% Triton X-100, the beads were eluted by boiling in 2× gel sample buffer, and subjected to SDS-PAGE. The proteins of interest were subjected to peptide mapping.

### 2.6. Fusion protein phosphorylation

Fusion protein (1–5 μg) was incubated in 100 μl phosphorylation buffer with 0.1 mM DTT, and 35 μM [$\gamma$-$^{32}$P]ATP (2000 cpm/pmol), 1 μl of $pp60^{c-src}$ kinase (Upstate Biotechnology) for 90 min at 30°C. The reaction was stopped by boiling in gel sample buffer. The fusion proteins were then subjected to SDS-PAGE and autoradiography.

### 2.7. Peptide mapping

The phosphorylated proteins were excised and digested with trypsin at 0.15 mg/ml; the resulting phosphopeptides were separated by electrophoresis and ascending chromatography and subjected to autoradiography as previously described [35].

### 2.8. Phosphorylation of dystrobrevin in pervanadate stimulated 293T cells

Myc-tagged dystrobrevin constructs subcloned in PRK5 were transfected into HEK-293 cells by calcium phosphate coprecipitation using 20 μg of DNA per 10-cm dish. Forty-eight hours following transfection the cells were harvested. Pervanadate stimulation of the cells was performed immediately prior to harvest: 0.3% hydrogen peroxide in 10 mM sodium orthovanadate was diluted 100-fold into the media and incubated at 37°C for 10 min. All plates were rinsed twice in warm PBS, and scraped into 150 μl of IPB+2% SDS, sonicated and boiled. After boiling, 750 μl of cold IPB+INH was promptly added and the final detergent concentration was adjusted to 1% Triton. After incubating 20 min on ice, the insoluble fraction was removed by centrifugation at $100\,000\times g$. The supernatant was precleared with 100 μl of a 2× slurry of protein A-Sepharose (Pharmacia), and then incubated with 5 μl of 9E10 anti-myc ascites [36] and 100 μl of the 2× Protein A slurry. After 3 h at 4°C, the beads were washed

3 times in IPB/1% Triton X-100, and eluted by boiling in gel sample buffer.

The immunoprecipitated proteins were subjected to SDS-PAGE, transferred to PVDF membranes (Millipore), and immunoblotted with polyclonal anti-phosphotyrosine antibodies at a 1:500 dilution or affinity purified anti-DHD antibodies at 1:10 000.

*2.9. Sample preparation and immunoblotting*

Homogenates were obtained by homogenizing various tissues in IPB supplemented with protease inhibitors, and clarifying by centrifugation for 20 min at $1000 \times g$ at 4°C. Muscle and brain homogenates were then centrifuged for 15 min at $100\,000 \times g$ at 4°C. The supernatant was retained as the cytosol, and the pellet, after rinsing once with IPB, was retained as the crude membrane pellet. Synaptic membranes were purified from electric organ and brain as described previously [18,37].

Protein concentration was determined by Coomassie protein assay (Pierce). Samples were subjected to SDS-PAGE, transferred to PVDF and immunoblotted using anti-PYCT or anti-DHD at 1:100 dilution, unless otherwise indicated, in the presence or absence of 0.5 μg/ml fusion protein, followed by HRP conjugated anti-rabbit antibodies (Amersham) and ECL detection (NEN Life Science). Where indicated, blots were stripped and reprobed according to the manufacturer's protocol (NEN Life Science).

*2.10. Immunohistochemistry*

An adult rat was sacrificed, the soleus muscle was dissected out and snap-frozen in an isopentane dry ice bath. The muscle was embedded in OCT medium (Tissue-Tek) and 8-μm sections were cut, washed with PBS and fixed in 2% paraformaldehyde/2% sucrose in PBS for 15 min. The sections were then permeabilized in 0.5% Triton in PBS for 10 min, blocked in 10% normal goat serum in PBS for more than 1 h at 37°C and then incubated in primary antibody at 1:50 dilution in 3% normal goat serum in PBS overnight at 4°C. The sections were then washed three times in PBS and then incubated with rhodamine anti-rabbit antibody and fluorescein α-bungarotoxin in 3% normal goat serum/PBS for 1 h at room temperature. After washing extensively with PBS, sections were mounted in Immunon containing 30 μg/ml 1,4-diazabicyclo [2.2.2]-octane and viewed on a Zeiss immunofluorescence microscope. All steps were performed at room temperature unless otherwise indicated.

*2.11. Co-immunoprecipitation of dystrobrevin with syntrophin*

Crude rat brain homogenates (750 μg) were solubilized in 1 ml of 2% Triton/IPB+INH on ice for 20 min. After centrifugation at 40 000 rpm for 10 min at 4°C in a TLA 100.3 rotor, 3 μg of anti-syntrophin antibody and 100 μl of a 2× slurry of anti-mouse IgG Sepharose (Sigma) was added to the supernatant, and incubated 3 h with rocking at 4°C. After washing twice with IPB+500 mM NaCl+1% Triton X-100, and twice with IPB+1% Triton X-100, the bound proteins were eluted with gel sample buffer and subjected to SDS-PAGE, transferred to PVDF and immunoblotted as described above.

## 3. Results

*3.1. Identification of the tyrosine phosphorylation sites of dystrobrevin*

Dystrobrevin is a major tyrosine phosphorylated protein in *Torpedo* electric organ [18]. As shown in Fig. 1, it is comprised of a region homologous to the CRCT of dystrophin and the PYCT, which contains several phosphotyrosine consensus sites [18]. To identify the sites of dystrobrevin phosphorylation in *Torpedo*, dystrobrevin was phosphorylated by endogenous kinases present in *Torpedo* electric organ synaptic membranes by incubating the membranes with [$\gamma$-$^{32}$P]ATP. Phosphorylated dystrobrevin was immunoprecipitated (Fig. 2A) and digested with trypsin. The resulting phosphopeptides were resolved by two-dimensional phosphopeptide mapping which revealed three major phosphopeptides (Fig. 2B).

Because the consensus sites for tyrosine phosphorylation were present in the PYCT region of dystrobrevin, a glutathione-*S*-transferase-fusion protein encoding the PYCT was generated, phosphorylated in vitro using the tyrosine kinase, pp60$^{c-src}$, and subjected to phosphopeptide mapping. The resulting phosphopeptide map contained four reproducible major phosphopeptides (Fig. 2C, and schematically, Fig. 2D), including three which comigrated with phosphopeptides obtained by phosphorylation of native dystrobrevin with *Torpedo* synaptic kinases. These findings suggested that the major sites of dystrobrevin tyrosine phosphorylation are contained within the PYCT.

To determine the exact sites of phosphorylation, fusion proteins containing single tyrosine to phenylalanine mutations were constructed, phosphorylated and subjected to peptide mapping. As shown in the lower panels of Fig. 2B, mutation of Tyr-685 to phenylalanine eliminated phosphopeptide 4. In addition, mutation of Tyr-693 to phenylalanine eliminated phosphopeptide 3 while mutation of Tyr-710 to phenylalanine resulted in the removal of phosphopeptides 1 and 2 (Fig. 2F,G). These results indicated that Tyr-693 and Tyr-710 are the major sites of tyrosine phosphorylation by endogenous synaptic tyrosine kinases. Tyr-685, although not highly phosphorylated in synaptic membrane preparations in vitro, may yet represent an additional target for tyrosine kinases in vivo.

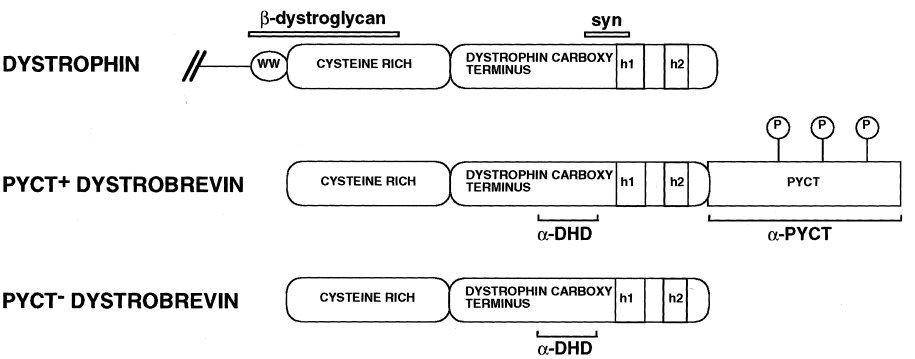


Fig. 1. Domains of dystrobrevin and the corresponding region of dystrophin. Dystrobrevin shows sequence homology to the cysteine rich region and carboxy terminus (CRCT) of dystrophin, defining it as a member of the dystrophin family. The carboxy terminus contains two regions predicted to form α-helices, denoted h1 and h2. The regions shown to interact with β-dystroglycan and syntrophin are indicated. *Torpedo* dystrobrevin and some mammalian splice variants of dystrobrevin (PYCT$^+$) have a unique C-terminus containing tyrosine phosphorylation consensus sites, while others do not (PYCT$^-$). The fusion proteins used to generate the anti-DHD (dystrophin homologous domain) and anti-PYCT (phosphotyrosine containing tail) antisera are bracketed.

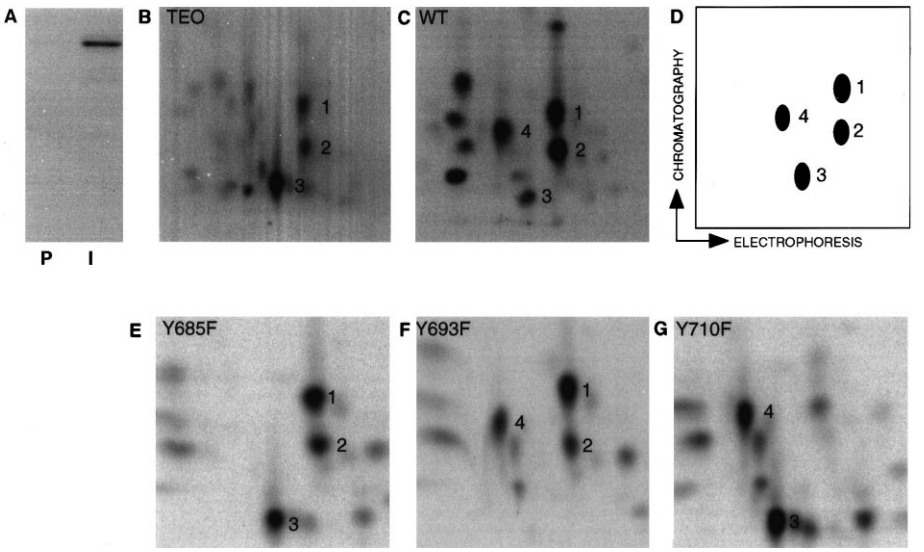


Fig. 2. Determination of the tyrosine phosphorylation sites on *Torpedo* dystrobrevin. A: Immunoprecipitation. *Torpedo* electric organ postsynaptic membranes (1 mg) were phosphorylated in vitro by endogenous kinases using [$\gamma$-$^{32}$P]ATP and solubilized. Dystrobrevin was immunoprecipitated using anti-DHD antibodies (I) or pre-immune serum (P), subjected to SDS-PAGE, and visualized by autoradiography. B–G: Phosphopeptide analysis. Following phosphorylation and immunoprecipitation, $^{32}$P-labeled dystrobrevin was digested with trypsin and the resulting phosphopeptides were separated by electrophoresis in one dimension and ascending chromatography in the second. To map the sites of phosphorylation, wild-type (C) and mutant (E–G) fusion proteins corresponding to the PYCT domain of *Torpedo* dystrobrevin were constructed. Purified fusion proteins were phosphorylated in vitro by recombinant *src* protein kinase, subjected to SDS-PAGE, autoradiography and trypsin digestion. The resulting phosphopeptides were analyzed as above. The four major phosphopeptides are depicted schematically (D).

### 3.2. Phosphorylation in 293T cells

To determine whether the tyrosine residues identified as sites of phosphorylation in vitro were also phosphorylated in intact cells, myc-tagged *Torpedo* dystrobrevin was expressed in 293T cells (Fig. 3). Dystrobrevin did not appear to be basally tyrosine phosphorylated in 293T cells. However, treatment of myc-dystrobrevin transfected 293T cells with the protein tyrosine phosphatase inhibitor, pervanadate, dramatically increased the phosphotyrosine content of dystrobrevin. Moreover, deletion of the PYCT region from dystrobrevin eliminated tyrosine phosphorylation in this system. Interestingly, Tyr-693 seemed to be the major site of phosphorylation in pervanadate treated 293T cells since mutation of this tyrosine to phenylalanine consistently abolished most of the observed tyrosine phosphorylation of dystrobrevin (myc-87Y693F). Mutation of Tyr-685 also reduced dystrobrevin phosphorylation. Thus, in 293T cells, as in electric organ, the PYCT is the major site of tyrosine phosphorylation.

### 3.3. Tissue and subcellular distribution of dystrobrevin

While dystrobrevin is a major tyrosine phosphorylated protein in *Torpedo* electric organ, the PYCT, and hence the potential for regulation by tyrosine phosphorylation, is not present in all splice variants of mammalian dystrobrevin (see Fig. 1). In order to examine the distribution of PYCT$^-$ and PYCT$^+$ dystrobrevin, we immunoblotted homogenates of various rat tissues with antibodies directed toward either the dystrophin homologous domain (anti-DHD) or the PYCT (anti-PYCT) (see Fig. 1). Neither antibody is specific for a particular isoform (i.e. they are insensitive to various splicing within the CRCT) and the anti-DHD antibody may cross-react with the closely related β-dystrobrevin; nonetheless, the anti-DHD antibody recognizes both PYCT$^-$ and PYCT$^+$ isoforms, while the anti-PYCT antibody recognizes only PYCT$^+$ isoforms.

As shown in Fig. 4, both antibodies recognized a 97-kDa species in *Torpedo* electric organ homogenate (TEO). In rat, the predominant isoform recognized by the anti-DHD antibody was 62 kDa which is expressed at similar levels in all

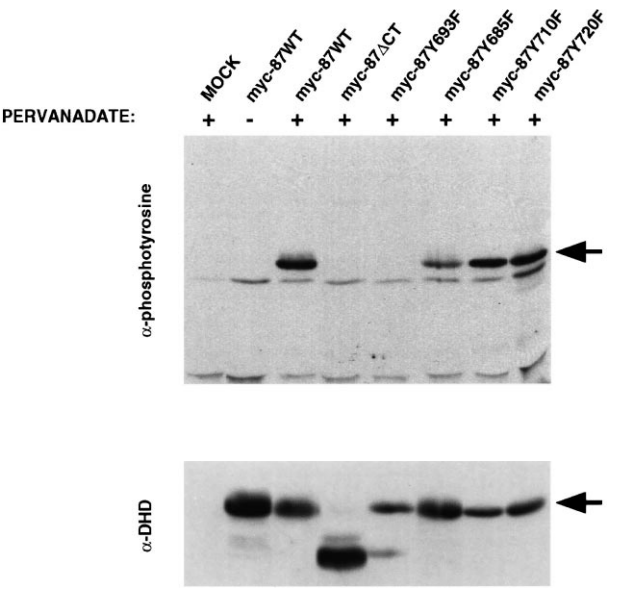


Fig. 3. Phosphorylation of dystrobrevin transiently expressed in HEK-293 cells. HEK-293 cells were either mock transfected or transiently transfected with the indicated wild-type or mutant myc-tagged *Torpedo* dystrobrevin cDNAs. Cells were treated with (+) or without (−) pervanadate for 10 min (unless otherwise indicated), lysed and immunoprecipitated with anti-myc antibodies. After resolution with SDS-PAGE and transfer to a PVDF membrane, immunoblotting was performed with anti-phosphotyrosine antibodies (top panel). Subsequently, the PVDF was stripped and reprobed with anti-dystrobrevin antibodies to assess levels of expression (bottom panel).

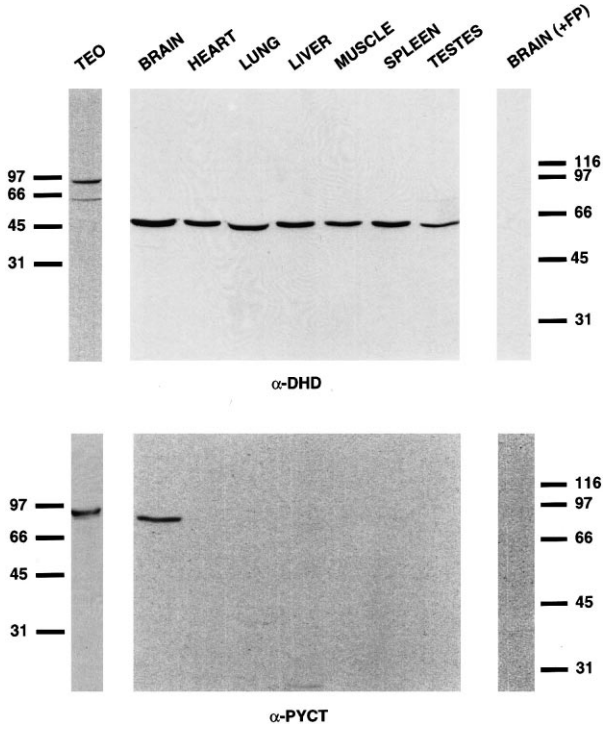


Fig. 4. Distribution of dystrobrevin isoforms in various tissues. Five micrograms of rat tissue homogenates, or 5 μg (top) and 0.1 μg (bottom) of *Torpedo* electric organ synaptic membranes (TEO) were subjected to SDS-PAGE, transferred to PVDF membranes and immunoblotted with anti-DHD (top) or anti-PYCT (bottom) antibodies. These signals were blocked by preincubation of the antibody with 3 μg/ml of the fusion protein used to generate the antibody (+FP). Molecular weight markers are indicated.

tissues. The predominant isoform recognized by the anti-PYCT antibody, on the other hand, was a 90-kDa protein in brain (Fig. 4, lower panel) with a 97-kDa protein also detected in skeletal muscle with longer exposures. Consistent with the complex distribution of dystrobrevin splice variants by Northern analysis [19,20], multiple other PYCT$^+$ and PYCT$^-$ isoforms could also be detected with long exposures and increased antibody concentrations (data not shown). Under such conditions, the anti-DHD antibody recognized the 90-kDa and 97-kDa isoforms; the anti-PYCT antibody, on the other hand, did not react with the 62-kDa isoform under any conditions examined. The specificity of these interactions was confirmed by blocking them with the immunizing fusion proteins ((+FP), and data not shown).

The fact that higher antibody concentrations and exposure times were necessary for the detection of the 90- and 97-kDa PYCT$^+$ dystrobrevin isoforms by the anti-DHD antibody suggests that these isoforms are less abundant than the 62-kDa PYCT$^-$ isoform. Thus, it seems that PYCT$^-$ dystrobrevin is ubiquitously expressed at relatively high levels, while PYCT$^+$ dystrobrevin is expressed at much lower levels in a selective pattern, consistent with a more specialized role for this isoform.

To further characterize the distribution of dystrobrevin isoforms, homogenates (H) of electric organ (TEO), brain and muscle were subjected to subcellular fractionation (Fig. 5). Upon centrifugation, PYCT$^+$ isoforms showed greater affinity for the membrane fraction (M) in all three tissues (Fig. 5). The PYCT$^-$ isoforms, on the other hand, remained almost entirely with the cytosol (C), indicating that the PYCT$^+$ isoforms are preferentially membrane associated. The 45-kDa band recognized by the anti-DHD antibody in muscle also appeared in longer exposures of the blot shown in Fig. 4. It may represent a degradation product of the 62-kDa dystrobrevin isoform. Alternatively, its size is consistent with the dystrobrevin-δ splice variant described by Sadoulet-Puccio and others, which is highly expressed in cardiac and skeletal muscle [20].

### 3.4. *Association of PYCT$^+$ dystrobrevin with synaptic membranes*

To examine the association of PYCT$^+$ isoforms with synaptic membranes, *Torpedo* electric organ membranes were fractionated into non-synaptic, mixed, and synaptic membranes. Both the anti-DHD and anti-PYCT antisera recognized a 97-kDa isoform which was enriched in synaptic mem-

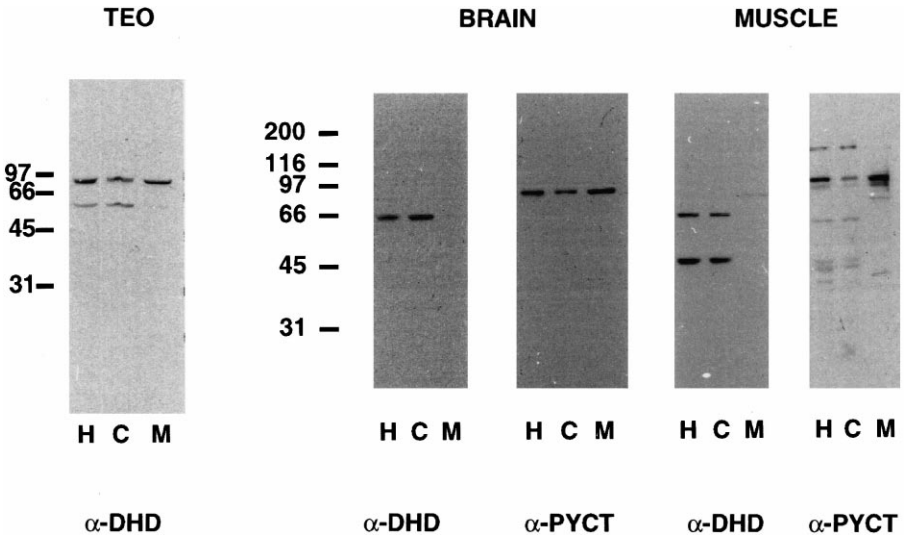


Fig. 5. Subcellular fractionation of dystrobrevin isoforms. Total homogenates (H) from *Torpedo* electric organ (TEO), rat brain or rat muscle were fractionated into membrane (M) and cytosol (C) components. Five micrograms of each were loaded per lane and subjected to SDS-PAGE and transferred to a PVDF membrane. Immunoblotting was performed using the anti-DHD or anti-PYCT antibodies as labeled. Molecular weight markers are indicated.

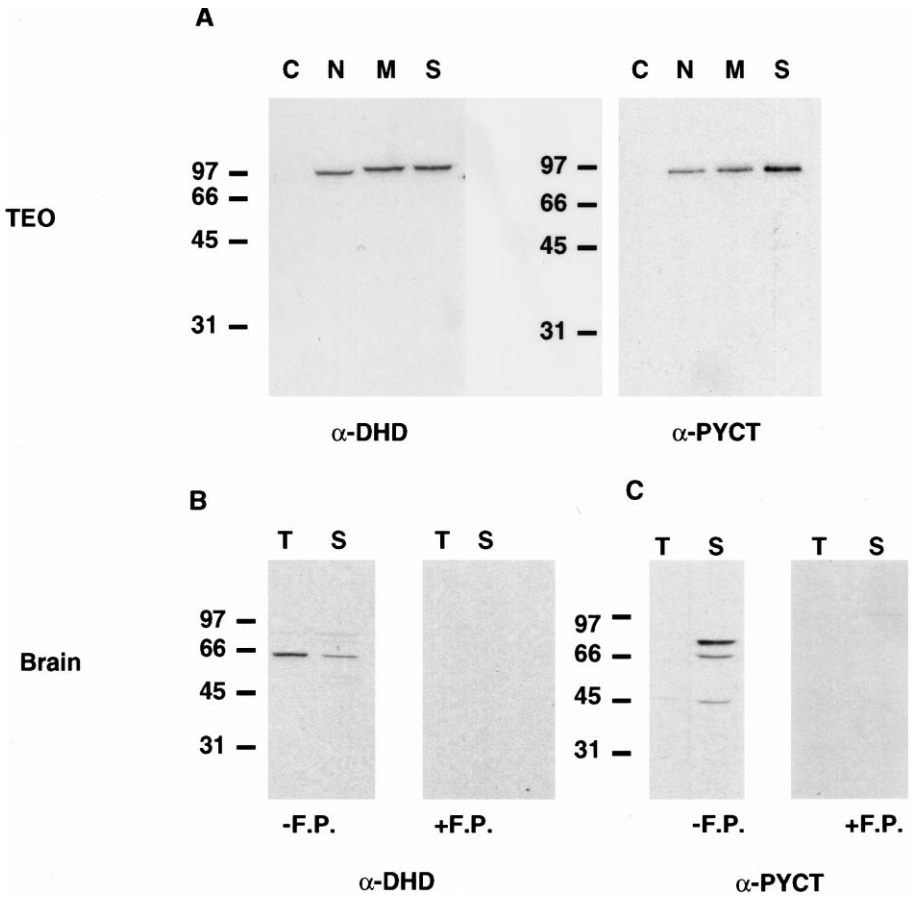


Fig. 6. Distribution of dystrobrevin isoforms in synaptic membranes. A: *Torpedo* electric organ homogenate was fractionated into cytosol (C) and crude membranes. The crude membranes were subjected to sucrose gradient sedimentation to yield non-synaptic (N), mixed (M) and synaptic (S) membranes. Western blotting was performed using anti-DHD antibodies (5 μg protein/lane) or anti-PYCT antibodies (0.2 μg protein/lane). The 97-kDa isoform, while present in all membrane fractions, is enriched in synaptic membranes. B: Synaptic membranes were prepared from crude rat brain membranes by sucrose gradient sedimentation (see Section 2.9). Five micrograms of either total (T) or synaptic membranes (S) were immunoblotted with the indicated antibodies in the absence (−FP) or presence (+FP) of 3 μg/ml fusion protein block. Molecular weight markers are indicated.

branes (Fig. 6A), as has been described previously [18]. To determine whether dystrobrevin was also enriched at central synapses, synaptic membranes were purified from total brain membranes. Fig. 6B shows that the 62-kDa dystrobrevin isoform, lacking the PYCT, was not enriched in synaptic membranes. On the other hand, the 90-kDa protein recognized by the anti-PYCT antiserum was greatly enriched in synaptic membranes relative to total membranes (Fig. 6C), the latter requiring longer exposure to detect the 90-kDa isoform (data not shown). Thus, in brain, as in electric organ, $PYCT^+$ isoforms are enriched in the synaptic membrane.

### 3.5. *Immunocytochemical localization of dystrobrevin in rat muscle*

Previous studies have shown that dystrobrevin in rat skeletal muscle is enriched at the NMJ, with lower levels throughout the sarcolemma [3]. To determine the localization of the $PYCT^+$ dystrobrevin isoform, adult rat muscle was double-labeled with both anti-PYCT antibody and α-bungarotoxin to localize the nicotinic acetylcholine receptors (Fig. 7). $PYCT^+$ dystrobrevin staining (α-PYCT) co-localized with α-bungarotoxin staining (α-BT), consistent with a synaptic localization for this isoform. The specificity of immunostaining is demonstrated by preadsorption of the antibody with the immunizing fusion protein (Fig. 7, α-BT and α-PYCT+FP).

### 3.6. *Co-immunoprecipitation with syntrophin*

The region of dystrobrevin which binds to syntrophin has been mapped within the CRCT (Fig. 1) [38–40]. To determine whether the PYCT domain altered the association of dystrobrevin with syntrophin, syntrophin was immunoprecipitated from rat brain homogenate using a monoclonal antibody which recognizes all three isoforms of syntrophin. Consistent with the results of Blake and others [19], the predominant isoforms co-immunoprecipitated with anti-syntrophin antibodies are the 90- and 97-kDa isoforms (Fig. 8, α-syn IP). However, the fact that only trace amounts of these isoforms relative to the 62-kDa $PYCT^-$ isoform were present in total rat brain homogenate (Fig. 8, LOAD), demonstrates that the 90-kDa and 97-kDa $PYCT^+$ isoforms are selectively co-immunoprecipitated with anti-syntrophin antibodies. Neither isoform is immunoprecipitated by a control monoclonal antibody (Fig. 8, cMAb IP). Stripping and reprobing this blot with anti-PYCT antibodies (Fig. 8, right panel) confirms that the 90- and 97-kDa but not the 62-kDa species contains the PYCT.

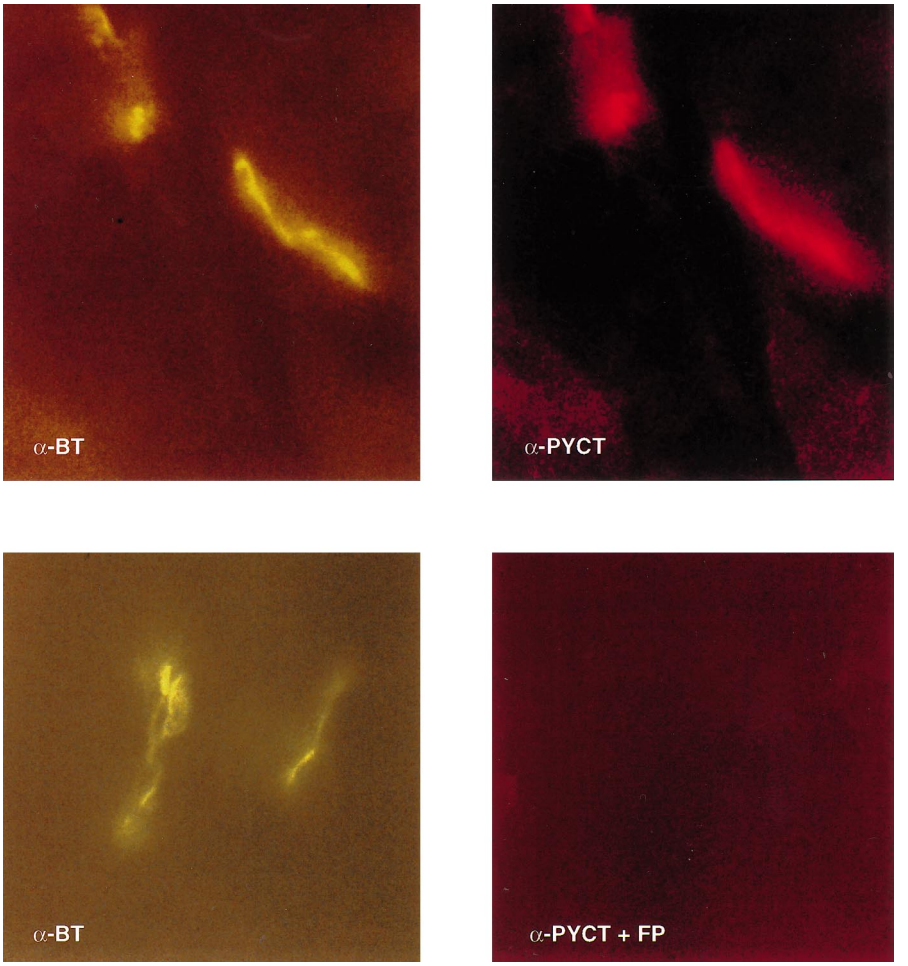


Fig. 7. Immunofluorescence of dystrobrevin in muscle. Muscle sections were double labeled with anti-PYCT antibodies followed by rhodamine-conjugated anti-rabbit antibodies and FITC conjugated α-bungarotoxin (top right and top left). Pre-incubation of the anti-PYCT antibodies with 1 μg/ml fusion protein abolished dystrobrevin staining (lower right) at the endplate visualized with FITC-α-bungarotoxin (lower left).

## 4. Discussion

The variety of isoforms which exist for many components of the dystroglycan complex suggests that the composition of the dystroglycan complex is highly regulated. By combining different isoforms, a variety of tissue and subcellular specific complexes could be constructed to play distinct functional roles. In particular, synapse specific dystrophin complexes may have special properties enabling them to modulate synaptic architecture. Here, evidence is presented that $PYCT^+$ dystrobrevin is a synapse specific isoform which is subject to modulation by tyrosine kinases.

The major sites of tyrosine phosphorylation of *Torpedo* dystrobrevin are Y693 and Y710, which are contained within the PYCT. Interestingly, those isoforms which contain the PYCT appear to be synapse specific. Immunoblots of various tissues demonstrate that the 62-kDa ($PYCT^-$) isoform of dystrobrevin is widely expressed, while the 90- and 97-kDa isoforms are restricted to brain and muscle. The difference between the 90- and 97-kDa isoforms is unclear but may be due to alternative splicing at a site outside of the PYCT or to post-translational modifications such as phosphorylation. Subcellular fractionation of *Torpedo* electric organ and rat brain show that the 62-kDa ($PYCT^-$) dystrobrevin is mostly soluble while the 90- and 97-kDa ($PYCT^+$) isoforms are enriched in synaptic membranes. Immunocytochemical staining of muscle shows that $PYCT^+$ isoforms of dystrobrevin are present at the neuromuscular junction, reminiscent of the synaptic distribution of the β2 isoform of syntrophin.

The studies presented here suggest that the presence of this synaptic form of dystrobrevin may alter the dystrophin complex in several ways. First, $PYCT^+$ isoforms seem to bind syntrophin in greater amounts or with higher affinity, since $PYCT^+$ isoforms are enriched in syntrophin preparations relative to $PYCT^-$ isoforms. These results are consistent with those of Blake et al. [19] which demonstrated that dystrobrevin 1 ($PYCT^+$) preferentially co-immunoprecipitated with brain syntrophin compared to dystrobrevin 2 ($PYCT^-$). Second, $PYCT^+$ isoforms are present in membrane fractions, suggesting that they have additional anchoring sites to the membrane, that they have a higher affinity for them, or that they are preferentially bound to isoforms of syntrophin which have greater membrane affinity.

Finally, the presence of the PYCT makes dystrobrevin an excellent candidate for regulation by tyrosine phosphorylation. Analysis of this alternatively spliced PYCT using an α-helical coiled-coil prediction program reveals a potential mechanism for the modulation of dystrobrevin function by tyrosine phosphorylation. Analysis of the sequence for PYCT itself shows that it has a relatively low propensity to

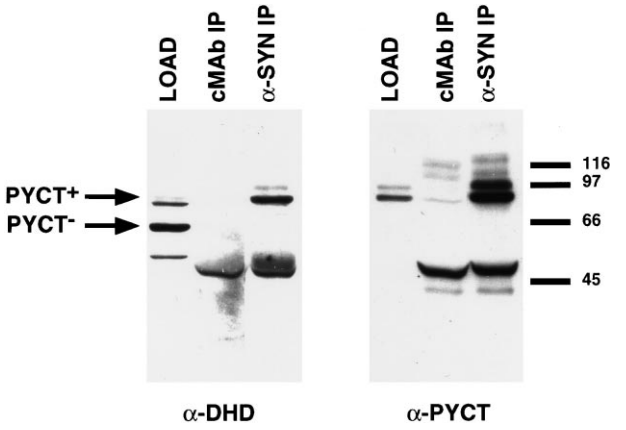


Fig. 8. Co-immunoprecipitation of dystrobrevin isoforms with syntrophin. Rat brain homogenates (LOAD) were solubilized (see Section 2) and subjected to immunoprecipitation with either a control monoclonal antibody (cMAb IP) or anti-syntrophin (α-syn IP). The immunoprecipitated proteins were subjected to SDS-PAGE, transferred to a PVDF membrane and subjected to immunoblotting using anti-DHD antibody. The blot was subsequently stripped and reprobed with anti-PYCT antibodies (right panel). The arrow shows the major species recognized by the anti-PYCT antibody. Molecular weight markers are indicated.

form coils (0.233). However, when tyrosines 693 and 710, the major sites of tyrosine phosphorylation identified in this paper, are converted to negatively charged amino acids, like glutamate, the propensity to form coils increases dramatically (0.999). This is particularly interesting given the finding that the CRCT present in dystrophin and other family members also contains two regions predicted to form coils (H1 and H2 in Fig. 1). It has previously been suggested that this region may mediate heteromeric or homomeric interactions between members of the dystrophin family [41]. If this is so, the phosphorylation of the C-terminus of dystrobrevin may increase its propensity to coil, creating a new binding site for other dystrophin family members.

Thus, $PYCT^+$ dystrobrevin isoforms are attractive candidates for modulation of the synaptic cytoskeleton. Tyrosine phosphorylation, induced by such mediators as agrin, may modulate the affinity of dystrobrevin for other proteins, resulting in alterations in synaptic structure. Moreover, the fact that $PYCT^+$ dystrobrevin is highly expressed in brain and enriched in synaptic membranes suggests that $PYCT^+$ dystrobrevin may also play a role in modulating synapses in the central nervous system.

*Acknowledgements:* We would like to thank Carol W. Doherty for her excellent technical assistance, Dr. Stanley Froehner for his generous gift of anti-syntrophin antibody, Michael Ehlers, Sunjeev Kamboj for critical reading of the manuscript and Doreen L. Bury for her excellent assistance in its preparation. This research was sponsored by an award from the National Institutes of Health, NS24418.

## References

[1] Jessell, T. and Kandel, E. (1993) Cell/Neuron 72/10, 1–30.
[2] Froehner, S.C. (1993) Annu. Rev. Neurosci. 16, 347–368.
[3] Carr, C., Fischbach, G.D. and Cohen, J.B. (1989) J. Cell Biol. 109, 1753–1764.
[4] Sealock, R., Butler, M.H., Kramarcy, N.R., Gao, K.X., Murnane, A.A., Douville, K. and Froehner, S.C. (1991) J. Cell Biol. 113, 1133–1144.
[5] Gautam, M., Noakes, P.G., Mudd, J., Nichol, M., Chu, G.C., Sanes, J.R. and Merlie, J.P. (1995) Nature 377, 232–236.
[6] Kramarcy, N.R., Vidal, A., Froehner, S.C. and Sealock, R. (1994) J. Biol. Chem. 269, 2870–2876.
[7] Butler, M.H., Douville, K., Murnane, A.A., Kramarcy, N.R., Cohen, J.B., Sealock, R. and Froehner, S.C. (1992) J. Biol. Chem. 267, 6213–6218.
[8] Froehner, S.C., Murnane, A.A., Tobler, M., Peng, H.B. and Sealock, R. (1987) J. Cell Biol. 104, 1633–1646.
[9] Ohlendieck, K., Ervasti, J.M., Matsumura, K., Kahl, S.D., Leveille, C.J. and Campbell, K.P. (1991) Neuron 7, 499–508.
[10] Hoffman, E., RH, B. and LM, K. (1987) Cell 51, 919–928.
[11] Koenig, M., Monaco, A.P. and Kunkel, L.M. (1988) Cell 53, 219–226.
[12] Ervasti, J.M. and Campbell, K.P. (1991) Cell 66, 1121–1131.
[13] Ibraghimov-Beskrovnaya, O., Ervasti, J., Leveille, C., Slaughter, C., Sernett, S. and Campbell, K. (1992) Nature 355, 696–702.
[14] Yang, B., Ibraghimov-Beskrovnaya, O., Moomaw, C.R., Slaughter, C.A. and Campbell, K.P. (1994) J. Biol. Chem. 269, 6040–6044.
[15] Yoshida, M., Yamamoto, H., Noguchi, S., Mizuno, Y., Hagiwara, Y. and Ozawa, E. (1995) FEBS Lett. 367, 311–314.
[16] Tinsley, J.M., Blake, D.J., Zuellig, R.A. and Davies, K.E. (1994) Proc. Natl. Acad. Sci. USA 91, 8307–8313.
[17] Love, D.R. et al. (1989) Nature 339, 55–58.
[18] Wagner, K.R., Cohen, J.B. and Huganir, R.L. (1993) Neuron 10, 511–522.
[19] Blake, D.J., Nawrotzki, R., Peters, M.F., Froehner, S.C. and Davies, K.E. (1996) J. Biol. Chem. 271, 7802–7810.
[20] Sadoulet-Puccio, H.M., Khurana, T.S., Cohen, J.B. and Kunkel, L.M. (1996) Hum. Mol. Genet. 5, 489–496.
[21] Peters, M., Adams, M. and Froehner, S. (1997) J. Cell Biol. 138, 81–93.
[22] Adams, M.E., Butler, M.H., Dwyer, T.M., Peters, M.F., Murnane, A.A. and Froehner, S.C. (1993) Neuron 11, 531–540.
[23] Ahn, A.H., Yoshida, M., Anderson, M.S., Feener, C.A., Selig, S., Hagiwara, Y., Ozawa, E. and Kunkel, L.M. (1994) Proc. Natl. Acad. Sci. USA 91, 4446–4450.
[24] Ahn, A.H., Freener, C.A., Gussoni, E., Yoshida, M., Ozawa, E. and Kunkel, L.M. (1996) J. Biol. Chem. 271, 2724–2730.
[25] Peters, M.F., Kramarcy, N.R., Sealock, R. and Froehner, S.C. (1994) NeuroReport 5, 1577–1580.
[26] Kleiman, R.J. and Reichardt, L.F. (1996) Cell 85, 461–464.
[27] McMahan, U. (1990) Cold Spring Harbor Symp. Quant. Biol. 55, 407–418.
[28] Reist, N.E., Werle, M.J. and McMahan, U.J. (1992) Neuron 8, 865–868.
[29] Wallace, B.G., Qu, Z. and Huganir, R.L. (1991) Neuron 6, 869–878.
[30] Ferns, M., Deiner, M. and Hall, Z. (1996) J. Cell Biol. 132, 937–944.
[31] Glass, D.J. et al. (1996) Cell 85, 513–523.
[32] DeChiara, T. et al. (1996) Cell 85, 1–20.
[33] Wagner, K.R., Mei, L. and Huganir, R.L. (1991) Curr. Opin. Neurobiol. 1, 65–73.
[34] Qu, Z.C., Moritz, E. and Huganir, R.L. (1990) Neuron 4, 367–378.
[35] Roche, K.W., O'Brien, R.J., Mammen, A.L., Bernhardt, J. and Huganir, R.L. (1996) Neuron 16, 1179–1188.
[36] Evan, G.I., Lewis, G.K., Ramsay, G. and Bishop, J.M. (1985) Mol. Cell. Biol. 5, 3610–3616.
[37] Blackstone, C.D., Moss, S.J., Martin, L.J., Levey, A.I., Price, D.L. and Huganir, R.L. (1992) J. Neurochem. 58, 1118–1126.
[38] Ahn, A.H. and Kunkel, L.M. (1995) J. Cell Biol. 128, 363–371.
[39] Dwyer, T.M. and Froehner, S.C. (1995) FEBS Lett. 375, 91–94.
[40] Suzuki, A., Yoshida, M. and Ozawa, E. (1995) J. Cell Biol. 128, 373–381.
[41] Blake, D.J., Tinsley, J.M., Davies, K.E., Knight, A.E., Winder, S.J. and Kendrick-Jones, J. (1995) Trends Biochem. Sci. 20, 133–135.